Research Article

Zhang Dai, Fangfang Yan, Mei Qin, and Xu Yan*

Fabrication of flexible SiO_2 nanofibrous yarn via a conjugate electrospinning process

https://doi.org/10.1515/epoly-2020-0063
received August 19, 2020; accepted September 17, 2020

Abstract: Nowadays, different kinds of polymers, including ceramics, are electrospun into fibrous materials with different structures by electrospinning. Generally, the as-spun ceramic fibers are randomly oriented membranes and brittle without flexibility. Here, we report the fabrication of flexible SiO_2 electrospun yarns using poly (vinyl alcohol) (PVA) as a template through a conjugate electrospinning process and calcination. It was found that the calcined as-spun fibers and yarns are obviously thinned with PVA component removal. Fourier transform infrared spectroscopy and energy-dispersive spectroscopy examinations suggested that the obtained yarn after calcination was SiO_2 yarn. The SiO_2 yarn showed good flexibility without cracking after 180° bending. The flexible ceramic yarn may have potential application in functional textiles.

Keywords: electrospinning, PVA, SiO_2, flexibility, nanofibrous yarn

1 Introduction

Nowadays, electrospinning is believed to be an effective and simple method to produce continuous functional fibrous materials. By electrospinning, different kinds of materials are electrospun into fibers, including both organic (1,2) and inorganic (3,4), with diameters ranging from subnanometers to several micrometers (5). These organic and inorganic as-spun fibrous materials have been applied in various fields such as thermal insulated sponges (6,7), filtration (8–10), stimuli-responsive materials (11), food packing (12), precursor fibers for carbon nanofibers (13), reinforced composites (14,15), drug carriers (16–18), actuators (19), wound care (20–23), smart textiles (24–26), and battery relative materials (27–29), partly due to their porous and designable structures (30–32).

Generally, electrospun fibrous materials were collected as a nonwoven mesh with fibers randomly arranged. After a thorough research, it was found that the structures of the as-spun fiber and fibrous materials may play important roles in their properties and applications (30–32). Consequently, more and more attention was paid to control and design the structures of the electrospun fibrous materials by modifying the spinnerets and collectors (32–35). Specific to the electrospun yarns, "conjugate electrospinning," with which two spinnerets are connected to two opposite polarity high-voltage supply, was found to be obtained through the electrospun fiber yarn in one step (36–39). By conjugate electrospinning, a series of polymer yarns as well as inorganic oxide arrays were fabricated (38–40). However, flexible inorganic yarns were rarely reported due to the complex process and brittleness.

Generally, the electrospun inorganic fibers are too brittle without flexibility. To overcome this disadvantage, researchers had found that using poly(vinyl alcohol) (PVA) or polyvinyl pyrrolidone (PVP) as template materials blended with inorganic salt gel could help to produce flexible ceramic nanofibrous mats via electrospinning process and calcination (41–44). Nevertheless, flexible inorganic nanofibrous yarn is still a challenge. This study reports on the fabrication of flexible SiO_2 nanofibrous yarn via a conjugate electrospinning process and calcination. The morphology, chemical structures, thermal stability, and flexibility of the prepared yarns are examined.

* **Corresponding author: Xu Yan,** Industrial Research Institute of Nonwovens & Technical Textiles, College of Textiles and Clothing, Qingdao University, Qingdao 266071, China; Collaborative Innovation Center for Eco-Textiles of Shandong Province, Qingdao University, Qingdao 266071, China; Shandong Center for Engineered Nonwovens, Qingdao University, Qingdao 266071, China; State Key Laboratory of Bio-Fibers and Eco-Textiles, Qingdao University, Qingdao 266071, China, e-mail: yanxu-925@163.com
Zhang Dai, Fangfang Yan, Mei Qin: Industrial Research Institute of Nonwovens & Technical Textiles, College of Textiles and Clothing, Qingdao University, Qingdao 266071, China

2 Materials and methods

2.1 Materials

PVA (M_w = 66,000), tetraethylorthosilica (TEOS; 98%), phosphoric acid (H_3PO_4, 85 wt%), and *N*,*N*-dimethylformamide were purchased from Aladdin Co., Ltd (Shanghai, China). Deionized water was made in lab. All the chemicals were used as received without further purification.

2.2 Preparation of electrospinning solutions

PVA was dissolved in deionized water at 11 wt% within a water bath at 40°C for 4 h and then cooled naturally. TEOS, H_3PO_4, and deionized water were mixed with a weight composition of TEOS:H_2O:H_3PO_4 = 1:1:0.02 according to previous studies (41,42) and stirred at room temperature for 4 h to form a uniform silica gel, as suggested in Figure 1a. Then, the prepared silica gel was dropped slowly into PVA solutions with a weight ratio of 1:1 and stirred for another 3 h to obtain the spinning precursor (41).

2.3 Fabrication of SiO_2 yarn

To produce SiO_2 yarn, conjugate electrospinning was processed with two parallel separated opposite-polarity high-voltage supply and vertically placed rotating trumpet collector as well as a rotating drum collector, as suggested in Figure 1b. During the conjugate electrospinning process, the prepared spinning precursor was loaded into two 5 mL syringes with a flat metal needle (18G, inner diameter: 0.9 mm), and then the two syringes were fixed onto the syringe pumps with a feed rate of 18 mL/min. The needles were connected to two opposite-polarity high-voltage supply (−30 kV–0 and 0–30 kV), respectively. The high voltages were set to be ±16 kV, respectively. The horizontal distance between the high voltage supply to the collector was set to be about 19 cm, and the vertical distance between the two collectors was about 20 cm. The electrospinning process was taken at an ambient temperature of 26°C and a humidity of 56%. The rotating drum collector was static, however, and the average collected yarn length was about 12 cm.

The collected PVA/silica yarns were placed in a ceramic ark and then put into the tube furnace. Afterward, the yarns were calcined in air with a heating rate of 3°C/min to 800°C and then kept at 800°C for 6 h to remove the organic components (41). After natural cooling, the inorganic SiO_2 yarns could be obtained.

2.4 Characterization

The morphology and the energy-dispersive spectroscopy (EDS) of the electropsun yarn were examined by a scanning electron microscope (SEM, Phenom Pro; Thermo Fisher Scientific). The average diameter of the as-spun fiber was measured through a soft: nano-measurement of 1.2 with ten yarns. The Fourier transform infrared spectroscopy (FTIR) spectra were characterized by a Thermo Scientific Nicolet iS10 spectrometer. The mechanical property of the fabricated yarns (5 cm length) was examined by a universal testing machine (Instron 3352) with a

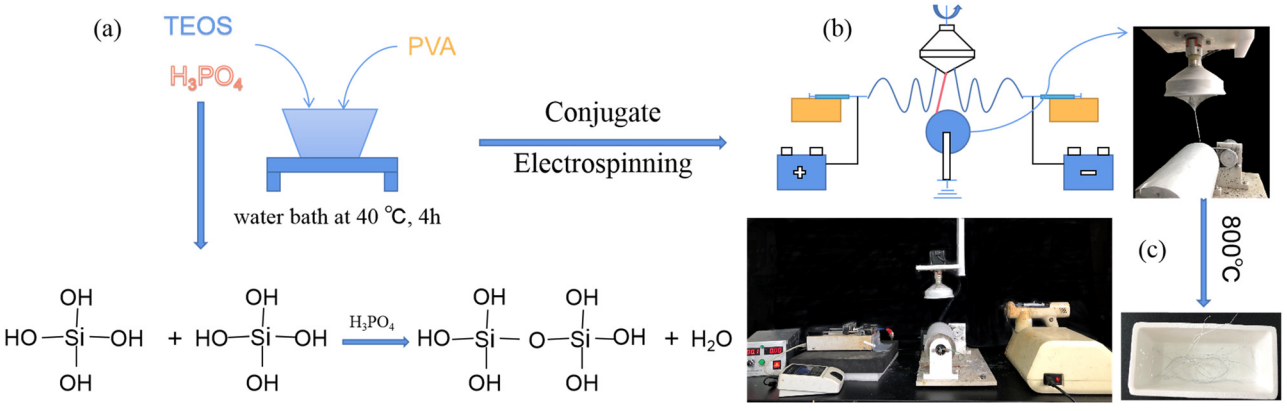

Figure 1: Schematic image of the preparation of spinning precursor (a), the fabrication of electrospun yarn by conjugate electrospinning process (b) and calcination of the as-spun yarn (c).

speed of 0.02 mm/min. The weight–temperature relationships of the yarns were tested through a thermal gravimetric analyzer (TGA/DSC3+, Mettler Toledo).

3 Results

The morphology of the fabricated yarn is shown in Figure 2. As can be seen in Figure 2a, the electrospun PVA/silica yarn with an average diameter of 199.77 ± 13.86 mm and a linear density of 14.8 tex had a relative uniform twisted structure with a little hairiness. The enlarged image in Figure 2c suggested that the electrospun fibers generally oriented well and had average diameters of about 380 ± 76 nm. After calcination, the yarn showed a more tight and lightly twisted structure without hairiness, and the yarn diameter was reduced to 128.96 ± 2.88 mm with the fiber diameters of about 315 ± 110 nm, as suggested in Figure 2b and d. Based on ten samples, after calcination, the reduction rate of the yarn diameters was found to be about 35.1%, while the fiber diameter reduced to about 17.3%. The reduction rate of the fiber diameter was nearly half of that of the yarns. It could be imagined that both the neighborhood fibers reduced due to the organic component removal after calcination, and then the extra space was filled by the calcined fibers.

We also examined the elements in the as-spun yarns. As shown in Figure 2e, there are mainly three elements in the PVA/silica yarn: carbon, oxygen, and silicon, While, after calcination, there are mainly oxygen and silicon elements (Figure 2f), which indicates that the organic components were removed during the calcination process and then only pure SiO_2 yarn remained.

Figure 3a shows the FTIR spectra of the prepared yarns before and after calcination. As can be seen from the spectra, the fabricated PVA/silica yarn showed typical PVA absorption peaks at 3,430 cm^{-1} (–OH), 2,930 cm^{-1} ($–CH_2$), and 1,720 cm^{-1} (C═O). There were also Si–O–Si bond absorption peaks at 1,080 cm^{-1}, 804 cm^{-1} as well as the Si–OH bond peaks at 963 cm^{-1}, suggesting the presence of silica in the as-spun yarn. After calcination, the PVA absorption peaks disappeared; only Si–O–Si absorption peaks could be found at 1,130 and 804 cm^{-1}, indicating the calcined yarn was SiO_2 yarn. Figure 3b presents the weight–temperature curve of the prepared yarns before and after calcination. For the as-spun PVA/silica yarn, as the temperature increased the yarn weight was reduced

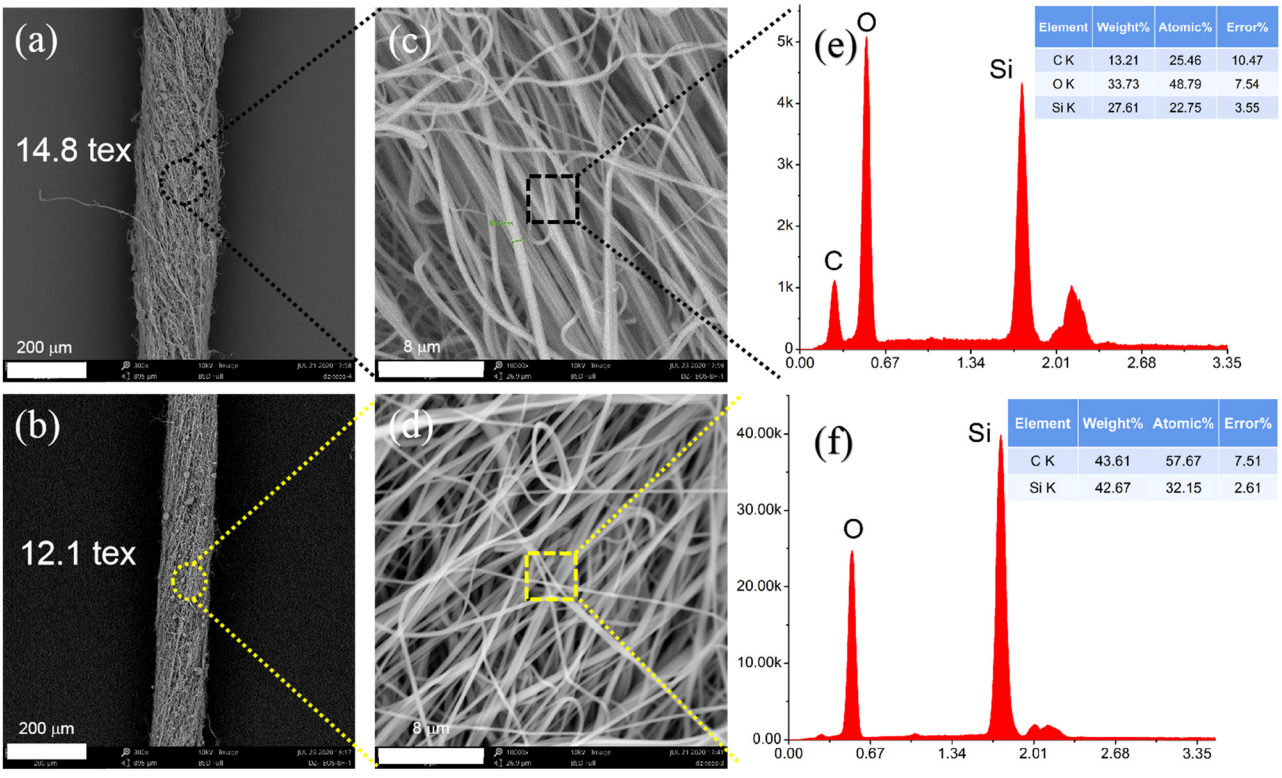

Figure 2: SEM images of the prepared yarns (a) PVA/silica, the PVA/silica fibers (c), the calcined yarn (b), the fibers in calcined yarn (d), as well as the EDS of the as-spun fibers before and after calcination (e and f), respectively.

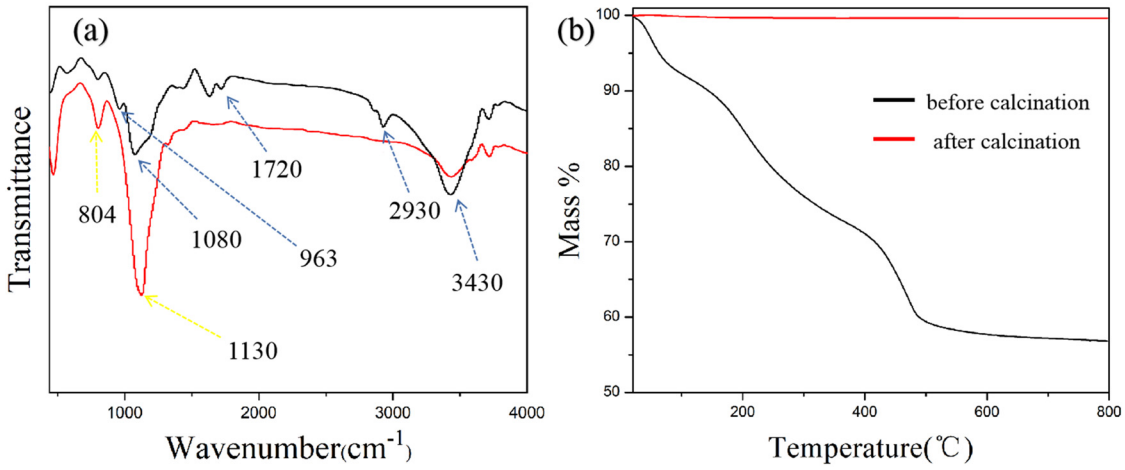

Figure 3: FTIR spectra (a) and the weight–temperature curve (b) of the PVA/silica yarns before and after calcination.

accordingly due to the PVA melt volatilization. When the temperature exceeded 500°C, the weight reduction was weakened, since the organic components almost completely evaporated. For the calcined yarn, the weight did not seem to change as the temperature increased.

As presented in Figure 4a, the tensile property of the prepared yarns before and after calcination was tested. It was found that the PVA/silica yarn showed a maximum stress of 3.8 MPa and maximum elongation to 0.32%. Once the PVA/silica yarn was broken, a few continuous fibers still remained, as suggested in the left inset image in Figure 4a. However, after calcination, the tensile property was obviously reduced to 1.5 MPa stress and about 0.03% strain. Once the calcined yarn was broken, one can find all the fibers were broken. The decreased strength of the calcined yarn may result from the brittle individual SiO_2 fiber. Since the organic component PVA was removed after calcination, the remaining SiO_2 formed a fiber with extremely small-sized crystal grains (41). In some sense, the SiO_2 fiber was not a continuous one. Consequently, its strength is weakened. Thankfully, the calcined yarn showed a certain flexibility, as suggested in Figure 4b–d. The calcined SiO_2 yarn could be bent without cracking. After bending, it could recover to the original form. From the SEM images before and after ten-circle bending, only a few fibers were broken, while the whole still retained the

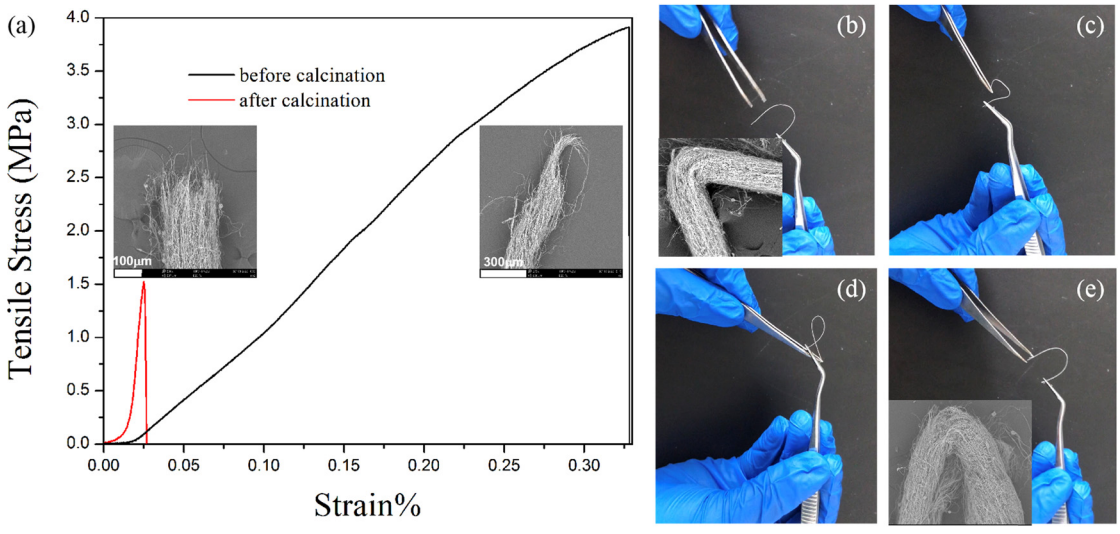

Figure 4: The mechanical property of the prepared yarns (a) with inset images of the broken yarns before and after calcination and the flexibility of the calcined yarn (b–d) with inset images of bending before and after ten circles.

yarn structure. The flexibility was believed to result from the one-dimensional (1D) silica nanofiber with extremely small-sized crystal grains (41).

4 Conclusions

In summary, we have successfully fabricated PVA/silica nanofiber yarn through a conjugate electrospinning process and then calcined the PVA/silica yarn in air at 800°C for 6 h to obtain the SiO_2 nanofiber yarn. The diameter of the calcined SiO_2 fiber and yarn was reduced up to 17.3 and 35.1%, respectively. The EDS, FTIR as well as the weight–temperature examination suggested that the calcined yarn was mainly SiO_2 yarn. Although the calcined SiO_2 yarn showed a significant weakness in the tensile property, it had good flexibility due to the extremely small size of the crystal grains in the nanofiber. Once the mechanical property was improved, the flexible inorganic yarns could be applied in the functional textiles.

Acknowledgments: This work was supported by the National Natural Science Foundation of China (51703102), the China Postdoctoral Science Foundation (2020M671998), State Key Laboratory of Bio-Fibers and Eco-Textiles (Qingdao University) No. ZKT35, and the Innovation and Entrepreneurship Training Program for College Students of Qingdao University (X2019110650078).

References

(1) Ding B. Functional polymeric micro/nano-fibrous materials. Acta Polym Sin. 2019;50(8):764–74. doi: 10.11777/j.issn1000-3304.2019.19069.
(2) Huang ZM, Zhang YZ, Kotaki M, Ramakrishna SA. Review on polymer nanofibers by electrospinning and their applications in nanocomposites. Compos Sci Technol. 2003;63(15):2223–53. doi: 10.1016/S0266-3538(03)00178-7.
(3) Wu H, Pan W, Lin D, Li H. Electrospinning of ceramic nanofibers: Fabrication, assembly and applications. J Adv Ceram. 2012;1(1):2:1–23. doi: 10.1007/s40145-012-0002-4.
(4) Ostermann R, Cravillon J, Weidmann C, Wiebcke M, Smarsly BM. Metal-organic framework nanofibers via electrospinning. Chem Commun. 2010;47(1):442–4. doi: 10.1039/c0cc02271c.
(5) Jian SJ, Zhu J, Jiang SH, Chen SL, Fang H, Song YH, et al. Nanofibers with diameter below one nanometer from electrospinning. RSC Adv. 2018;8(9):4794–802. doi: 10.1039/C7RA13444D.
(6) Jiang S, Chen Y, Duan G, Mei C, Greiner A, Agarwal S, et al. High-density fibrous polyimide sponges with superior mechanical and thermal properties. ACS Appl Mater Inter. 2020;12(16):19006–14. doi: 10.1021/acsami.0c02004.
(7) Jiang SH, Helfricht N, Papastavrou G, Greiner A, Agarwal S. Low-density self-assembled poly(*n*-isopropyl acrylamide) sponges with ultrahigh and extremely fast water uptake and release. Macromol Rapid Commun. 2018;39(8):1700838. doi: 10.1002/marc.201700838.
(8) Pu Y, Yang X, Zhang Y, Li L, Xie Y, He B, et al. Fabrication and characterization of highly oriented composite nanofibers with excellent mechanical strength and thermal stability. Macromol Mater Eng. 2020;305:1900691. doi: 10.1002/mame.201900691.
(9) Yang X, Pu Y, Zhang Y, Liu X, Li J, Yuan D, et al. Multifunctional composite membrane based on $BaTiO_3$@PU/PSA nanofibers for high-efficiency PM2.5 removal. J Hazard Mater. 2020;391:122254. doi: 10.1016/j.jhazmat.2020.122254.
(10) Wang N, Zhai Y, Yang Y, Yang X, Zhu Z. Electrostatic assembly of superwetting porous nanofibrous membrane toward oil-in-water microemulsion separation. Chem Eng J. 2020;354:463–72. doi: 10.1016/j.cej.2018.08.019.
(11) Molnar K, Jedlovszky-Hajdu A, Zrinyi M, Jiang SH, Agarwal S. Poly(amino acid)-based gel fibers with ph responsivity by coaxial reactive electrospinning. Macromol Rapid Commun. 2017;38(14):1700147. doi: 10.1002/marc.201700147.
(12) Zhao LY, Duan GG, Zhang GY, Yang HQ, He SJ, Jiang SH. Electrospun functional materials toward food packaging applications: A review. Nanomaterials. 2020;10(1):150. doi: 10.3390/nano10010150.
(13) Duan GG, Fang H, Huang CB, Jiang SH, Hou HQ. Microstructures and mechanical properties of aligned electrospun carbon nanofibers from binary composites of polyacrylonitrile and polyamic acid. J Mater Sci. 2018;53:1–11. doi: 10.1007/s10853-018-2700-y.
(14) Jiang SH, Chen YM, Duan GG, Mei CT, Greiner A, Agarwal S. Electrospun nanofiber reinforced composites: A review. Polym Chem-UK. 2018;9:2685–720. doi: 10.1039/C8PY00378E.
(15) Chen Y, Sui L, Fang H, Ding C, Li Z, Jiang S, et al. Superior mechanical enhancement of epoxy composites reinforced by polyimide nanofibers via a vacuum-assisted hot-pressing. Compos Sci Technol. 2019;174(12):20–6. doi: 10.1016/j.compscitech.2019.02.012.
(16) Duan GG, Bagheri ARR, Jiang SH, Golenser J, Agarwal S, Greiner A. Exploration of macroporous polymeric sponges as drug carriers. Biomacromolecules. 2017;18(10):3215–21. doi: 10.1021/acs.biomac.7b00852.
(17) Zhang J, Li S, Ju DD, Li X, Zhang JC, Yan X, et al. Flexible inorganic core-shell nanofibers endowed with tunable multicolor upconversion fluorescence for simultaneous monitoring dual drug delivery. Chem Eng J. 2018;349:554–61. doi: 10.1016/j.cej.2018.05.112.
(18) Wang K, Wen HF, Yu DG, Yang Y, Zhang DF. Electrosprayed hydrophilic nanocomposites coated with shellac for colon-specific delayed drug delivery. Mater Des. 2018;143:248–55. doi: 10.1016/j.matdes.2018.02.016.
(19) Liu L, Bakhshi H, Jiang SH, Schmalz H, Agarwal S. Composite polymeric membranes with directionally embedded fibers for controlled dual actuation. Macromol Rapid Commun. 2018;39(10):1800082. doi: 10.1002/marc.201800082.
(20) Liu GS, Yan X, Yan FF, Chen FX, Hao LY, Chen SJ, et al. In situ electrospinning iodine-based fibrous meshes for antibacterial

wound dressing. Nanoscale Res Lett. 2018;13:309. doi: 10.1186/s11671-018-2733-9.
(21) Dong WH, Liu JX, Mou XJ, Liu GS, Huang XW, Yan X, et al.Performance of polyvinyl pyrrolidone-isatis root antibacterial wound dressings produced in situ by handheld electrospinner. Colloid Surf B. 2020;188:110766. doi: 10.1016/j.colsurfb.2019.110766.
(22) Zhang J, Zhao YT, Hu PY, Liu JJ, Liu XF, Hu M, et al.Laparoscopic electrospinning for in situ hemostasis in minimally invasive operation. Chem Eng J. 2020;395:125089. doi: 10.1016/j.cej.2020.125089.
(23) Liu XF, Zhang J, Liu JJ, Zhou QH, Hu PY, Yuan Z, et al. Bifunctional CuS composite nanofibers via in-situ electrospinning for outdoor rapid hemostasis and simultaneous ablating superbug. Chem Eng J. 2020;401:126096. doi: 10.1016/j.cej.2020.126096.
(24) Tan C, Zhu H, Ma T, Guo W, Liu X, Huang X, et al. A stretchable laminated GNRs/BNNSs nanocomposite with high electrical and thermal conductivity. Nanoscale. 2019;11(43):20648–58. doi: 10.1039/C9NR06060J.
(25) Chen W, Huang G, Li X, Li Y, Wang H, Jiang H, et al. Revealing the position effect of an alkylthio side chain in phenyl-substituted benzodithiophene-based donor polymers on the photovoltaic performance of non-fullerene organic solar cells. ACS Appl Mater Interfaces. 2019;11(36):33173–78. doi: 10.1021/acsami.9b07112.
(26) Tan CX, Dong ZG, Li YY, Zhao HG, Huang XY, Zhou ZC, et al. A high performance wearable strain sensor with advanced thermal management for motion monitoring. Nat Commun. 2020;11(1):3530. doi: 10.1038/s41467-020-17301-6.
(27) Wang H, Wang X, Fan T, Zhou R, Li J, Long Y, et al. Fabrication of electrospun sulfonated poly(ether sulfone) nanofibers with amino modified SiO_2 nanosphere for optimization of nanochannels in proton exchange membrane. Solid State Ion. 2020;349:115300. doi: 10.1016/j.ssi.2020.115300.
(28) Wang H, Li X, Zhuang X, Cheng B, Wang W, Kang W, et al.Modification of nafion membrane with biofunctional SiO_2 nanofiber for proton exchange membrane fuel cells. J Power Sources. 2017;340(1):201–9. doi: 10.1016/j.jpowsour.2016.11.072.
(29) Yu JJ, Liu SW, Duan GG, Fang H, Hou HQ. Dense and thin coating of gel polymer electrolyte on sulfur cathode toward high performance li-sulfur battery. Compos Commun. 2020;19:239–45. doi: 10.1016/j.coco.2020.04.015.
(30) Yang G, Li X, He Y, Ma J, Ni G, Zhou S. From nano to micro to macro: Electrospun hierarchically structured polymeric fibers for biomedical applications. Prog Polym Sci. 2017;81:80–113. doi: 10.1016/j.progpolymsci.2017.12.003.
(31) Chen S, Liu GS, He HW, Zhou CF, Yan X, Zhang JC. Physical structure induced hydrophobicity analyzed from electrospinning and coating polyvinyl butyral films. Adv Cond Matter Phys. 2019;2019:1–5. doi: 10.1155/2019/6179456.
(32) Nicole E. Zander. Hierarchically Structured Electrospun Fibers. Polymers. 2013;5(1):19–44. doi: 10.3390/polym5010019.
(33) Zhou H, Shi Z, Wan X, Fang H, Yu DG, Chen X, et al. The relationships between process parameters and polymeric nanofibers fabricated using a modified coaxial electrospinning. Nanomaterials. 2019;9(6):843. doi: 10.3390/nano9060843.
(34) Duan GG, Greiner A. Air-blowing-assisted coaxial electrospinning towards high productivity of core/sheath and hollow fibers. Macromol Mater Eng. 2019;304(5):1800669. doi: 10.1002/mame.201800669.
(35) Cai M, Yuan D, Zhang X, Pu Y, Liu XF, He HW, et al. Lithium ion battery separator with improved performance via side-by-side bicomponent electrospinning of PVDF-HFP/PI followed by 3D thermal crosslinking. J Power Sources. 2020;461:228123. doi: 10.1016/j.jpowsour.
(36) Wei L, Qin XH. Nanofiber bundles and nanofiber yarn device and their mechanical properties: A review. Tex Res J. 2016;86(17):1885–98. doi: 10.1177/0040517515617422.
(37) Ali U, Zhou YQ, Wang XG, Lin T. Direct electrospinning of highly twisted, continuous nanofiber yarns. J Text I. 2012;103(1):80–8. doi: 10.1080/00405000.2011.552254.
(38) He JX, Zhou YM, Qi K, Wang LD, Li PP, Cui SZ. Continuous Twisted Nanofiber Yarns Fabricated by Double Conjugate Electrospinning. Fiber Polym. 2013;14(11):1857–63. doi: 10.1007/s12221-013-1857-x.
(39) Sun F, Qi HN, Xie YR, Ma QL, He W, Xu D, et al. Flexible self-supporting bifunctional $[TiO_2/C]//[Bi_2WO_6/C]$ carbon-based Janus nanofiber heterojunction photocatalysts for efficient hydrogen evolution and degradation of organic pollutant. J Alloy Compd. 2020;830:154673. doi: 10.1016/j.jallcom.2020.154673.
(40) Sheng YQ, Tian J, Xie YR, Yang XL, Qi H, Ma QL, et al. Neoteric conjugative electrospinning towards alloplastic nanofiber yarns affording enhanced upconversion luminescence and tailored magnetism. ChemNanoMat. 2020;6:298–307. doi: 10.1002/cnma.201900621.
(41) Guo M, Ding B, Li X, Wang X, Yu J, Wang M. Amphiphobic nanofibrous silica mats with flexible and high-heat-resistant properties. J Phys Chem C. 2010;114(2):916–21. doi: 10.1021/jp909672r.
(42) Mao X, Si Y, Chen Y, Yang L, Zhao F, Ding B, et al. Silica nanofibrous membranes with robust flexibility and thermal stability for high-efficiency fine particulate filtration. Rsc Adv. 2012;2(32):12216–23. doi: 10.1039/c2ra22086e.
(43) Mao X, Bai Y, Yu J, Ding B. Flexible and highly temperature resistant polynanocrystalline zirconia nanofibrous membranes designed for air filtration. J Am Ceram Soc. 2016;99(8):2760–68. doi: 10.1111/jace.14278.
(44) Han WD, Ding B, Park M, Cui FH, Chae SH, Kim HY. Insight into the precursor nanofibers on the flexibility of La_2O_3-ZrO_2 nanofibrous membranes. e-Polymers. 2017;17(3):243–8. doi: 10.1515/epoly-2016-0088.